

# Comparative design and modeling study of single sided linear planner Switched reluctance motor

Zaafrane Wajdi, Khediri Jalel, Rehaoulia Habib  
High school of Sciences and Technology of Tunis (ESSTT)  
University of Tunis  
5 av. Taha Hussein BP 56 – 1008  
Tunis  
[wajdi.zaafrane@gmail.com](mailto:wajdi.zaafrane@gmail.com)

*Abstract:* - This paper presents the comparison study between two design method of a single sided Linear Planner Switched Reluctance Motor (LPSRM) with an a translator and a passive stator .The work presents a LSRM complete design by 2-D Finite Element Analysis method (2-D FEA) and rotary to linear conversion method design . A detailed analysis of the influence of various geometrical parameters on the force developed by the actuator mainly gives in particular tooth size influence on fixed and mobile parts. A model of the actuator is performed neglecting magnetic saturation. The proposed actuator can be used in positioning task for high precision application.

*Key-Words:* - Linear switched reluctance motor- single sided planner actuator- Rotary to linear switched reluctance motor conversion-optimal design-2D finite element analysis-LSRM modeling .

## 1 Introduction

Linear motor (LM) is an important device wish is usually used in many industrial applications because they reduce mechanical subsystems need or rotary-to-linear motion converter.

These actuators converts the converts the output mechanical power directly to linear motion in order to reduce friction and maintain problems and increase performance.

To perform linear motion with linear motor there is a different structure and technologies. LM can be an induction or a synchronous motor with a transverse or longitudinal flux. Also these actuators have several topologies which they can be with long or with short stator, double or single structure.

Furthermore LM can be with active translator and passive stator or active stator and passive translator.

In this work we studied a Linear Switched Reluctance Motor (LSRM) which is the counterpart of the rotating switched reluctance machine. In fact the LSRM is an electromechanical actuator composed by a fixed part and a toothed sliding part on rail.

This type of actuator is characterized by its simple structure and low construction cost, LSRM contains only concentrated windings on the stator or translator so it's easy to control. There are many varieties of LSRM such as planer structure, with single or double inductor, or tubular structure [11].

In addition there are two distinctive configuration; longitudinal flux or transverse flux who have been explored in detail in [2],[5]and[3].

LSRM provide a solution to wide verities industrial needs especially for the high precision manufacturing and robotic industry. This kind of actuator is combined with low and high speed transit application. More ever LSRM applications are varied and cover large areas such as: biomedical (motorization of pump syringe) [12] , position control [13] , railway vehicle [14], vertical elevator [15].

This actuator has a special and exceptional geometric which attracts a lots of researches in terms of modeling, analysis, design and control of the actuator [4].

Up to now, there is no LSRM conventional or standard methods design and this due to the complexity and to the different topologies and shapes of the actuator. LSRM design is done by various methods: the analytical method [3], 2D finite element analysis [16] and [7], the method of network reluctances [14] or by conversion rotary switched reluctance motor (RSRM) to LSRM [2] and [6].

Reference [7] studies the air gap influence on the force by the finite element method, reference [3] presents too a detailed analysis of the influence of different geometrical parameters on the performance

of LSRM double inductor for different values the current density ( $J$  varying from 5 to 15 A / mm<sup>2</sup>). The pole arc sensitivity on average torque of RSRM which is similar to LSRM is extensively studied in literature, the references [7], [8] and [9], studies the pole arc sensitivity by using 2-D FEA.

The objective of this paper is an optimum design of a single sided planner LSRM. This study gives a detailed analysis of the various geometrical parameters influence on the developed force by the actuator, in particular tooth size influence on stator and mobile parts. Rotary to linear conversion method is firstly done to design the actuator. Secondly 2D-FEA has used to check proposed method efficiency and ensure an optimum design. The second part of this work consists of modelling the LSRM without taking into account magnetic saturation.

## 2 Planner Linear Switched Reluctance Motor

In this work we study a planner longitudinal linear switched reluctance motor with an active mover and a passive stator which is composed by four phases. This configuration contain 8 translator pole and this similar to 8/6 (8 stator and 6 rotor poles) RSRM.

LSRM is composed by two elements the first one is a toothed magnetic material fixed to a support and called stator. The second is a sliding part by rails and is called the mover (translator).

This latter is formed by a different modules regularly distributed lodging the winding. This topology is a single sided LSRM with active translator and passive stator, figure (1). The stator windings are laminated with a copper and excited by a DC currents.

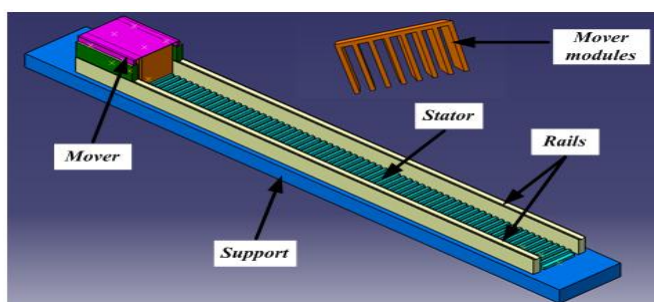


Figure 1: LSRM configuration

Initially two translator poles are aligned to the

two stator pole; another set of translator pole is out of alignment with respect to a different set of stator poles. The winding excitation sequences in the increasing inductance region make the translator move. The lack of non-magnetic separations between the different modules creates a radial magnetic flux path, this configuration is called longitudinal flux configuration.

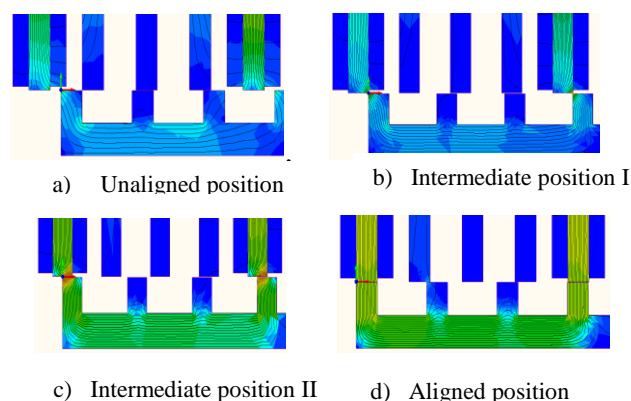


Figure 2: Magnetic flux path and field density for different translator position regions

Figure (2) show the magnetic flux path in a four different translator positions that are parallel to motion line. It is clear from figure (2, a) that the flux path in the unaligned position is very difficult to predict, thus the complexity of the steady state performance evaluation. The flux leakage in the aligned position shown in figure (2, d) is practically negligible, also we can see that there are two stator teeth aligned with mover teeth and other which are unaligned.

With an examination of these figures, it is observed that there is a local saturation occurs on stator tips and translator pole. This local saturation occurs when the relative positions of translator and stator pole is threshold of overlap or during partial overlap. In this region, the flux density is assumed to be the maximum value.

## 3 Rotary to linear switched reluctance motor design

To guarantee a good actuator operation and an optimum force characteristic per unit volume firstly the LSRM design of the is based on an equivalent RSRM that is more easily and more studied in numerous work (2),(6).

The RSRM conversion to LSRM has the advantage to use the knowledge base of the designers on rotary motor to design a linear motor this method will be validated by 2D-FEA to have a final optimized design. The design is transformed back in the linear domain and its compared with 2D-FEA. Some parameters are initially sited like current density value and the air gap how are selected as  $j = 5A/mm^2$  and  $e = 0.1mm$ . Stator and rotor pole width are sited as  $\beta_r = \beta_s = 18^\circ$

In order to obtain a small displacement in every step tooth pitch is chosen as  $\lambda = 10mm$ . The stator slot width must be greater than the translator slot width in order to impose a regular shift so:

$$w_{ss} = w_{ts} + \frac{\lambda}{3} \quad (1)$$

The material witch used is a 1010 steel this later admits a characteristic  $B = f(H)$  as it shown in figure (3)

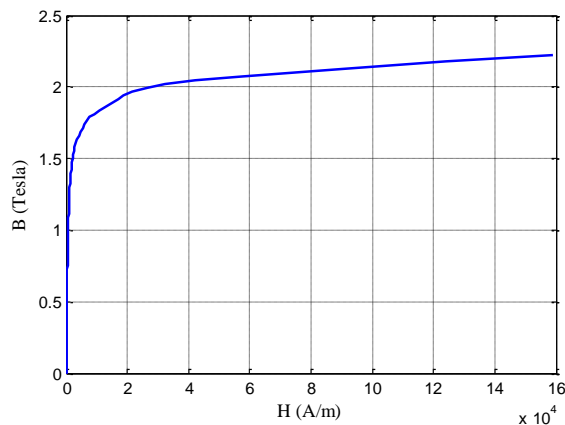


Figure 3:  $B = f(H)$  characteristic

The first stage of the design is based on the power expression to design an equivalent RSRM characterized by stator pole  $\beta_s$ , rotor pole  $\beta_r$  and a diameter bore as it gives by:

$$P = K_e K_d K_1 K_2 B_g A_{sp} D^2 L N_r \quad (2)$$

$$D = \sqrt{\frac{P \pi}{60 K_e K_d K_1 K_2 K B_g A_{sp} v_m}} \quad (3)$$

Where  $P$  means the output power of the LSRM,  $k_e$  the efficiency has defined to be equal to 40%,  $k_d$  is the phase duty cycle,  $k_1 = \frac{\pi^2}{120}$ ,  $k_2 = 0.7$  is a variable dependent on

the motor operating point, and  $k = 0.8$  is the ratio of stack length of the motor to its bore diameter.  $B_g = 2.2T$  is the air gap flux density (T),  $A_{sp} = 2e^4$  is the specific electric loading and  $v_m = 1.5(m/s)$  is the motor velocity.

The desired output power and output force are:

$$F_a = M_t a = 5 * 3 = 15N \quad (4)$$

$$P = F_a v_m = 10 * 1 = 15W \quad (5)$$

Where  $M_t$  is the mover weight (Kg) and  $a$  is the acceleration. ( $m/s^2$ )

### 3.1 Stator size design

The translator teeth width is obtained by RSRM conversion to LSRM method as follow:

$$W_{sp} = \frac{D \beta_r}{2} = \frac{25.5 * 0.314}{2} = 4mm \quad (6)$$

The stator slot width is obtained as:

$$W_{ss} = \frac{(\pi D - 6W_{tp})}{6} = \frac{(\pi * 25.5 - 6 * 4)}{6} = 9.3mm \quad (7)$$

The stator height teeth determination by the RSRM conversion to LSRM method is done as follows:

$$h_r = \frac{D}{2} - g - C_{ry} = \frac{25.5}{2} - 0.1 - 5 = 7.6mm \quad (8)$$

The stator yoke thickness is calculated by the RSRM conversion to LSRM method as follows:

$$C_{sy} = W_{sp} = \frac{D \beta_r}{2} = \frac{25.5 * 0.314}{2} = 4mm \quad (9)$$

### 3.2 Translator size design

In order to optimize the stator and translator teeth width and to simplify the study, we considered

$$W_{sp} = W_{tp} = 4mm \text{ consequently } \alpha = \frac{W_{tp}}{\lambda_t} = \frac{W_{sp}}{\lambda_s}$$

The translator slot width is calculated by the conversion RSRM to LSRM method as follows:

$$W_{ts} = \frac{(\pi D - 8W_{tp})}{8} = \frac{(\pi * 25.5 - 8 * 4)}{8} = 6mm \quad (10)$$

The height translator teeth determination is the result of RSRM conversion to LSRM method by this expression:

$$h_t = \frac{D_0}{2} - \frac{D}{2} - C_{sy} = \frac{90}{2} - \frac{25.5}{2} - 5 = 27.25mm \quad (11)$$

The translator yoke thickness is calculated by the RSRM conversion to LSRM by this expression:

$$C_{ty} = W_{tp} = \frac{D \beta s}{2} = \frac{25.5 * 0.314}{2} = 4mm \quad (12)$$

### 4 2-D FEA design

The LSRM 2D-FEA complete design method is summarized in the following organization chart where in every stage each geometric parameter is treated apart in order to choose the optimal value that ensures maximum force.

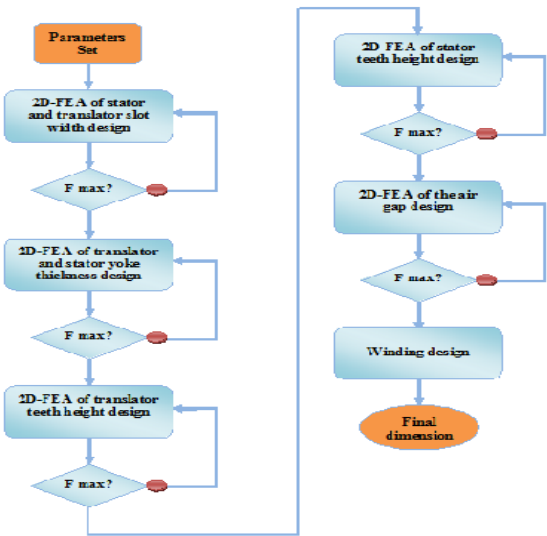


Figure 4: Organization chart of design method

#### 4.1 Translator and stator teeth width 2D-FEA analysis

In order to optimize the stator and translator teeth width and to simplify the study, we considered

$$W_{sp} = W_{tp} \text{ consequently } \alpha = \frac{W_{tp}}{\lambda_t} = \frac{W_{sp}}{\lambda_s}$$

The other parameters are set constant ( $h_{tp} = 25mm, h_{sp} = 5mm, C_{ry} = C_{sy} = 5mm, g = 0.1mm$ )

The analysis' is done with  $\alpha$  vary from  $0.1 * \lambda$  to  $0.6 * \lambda$

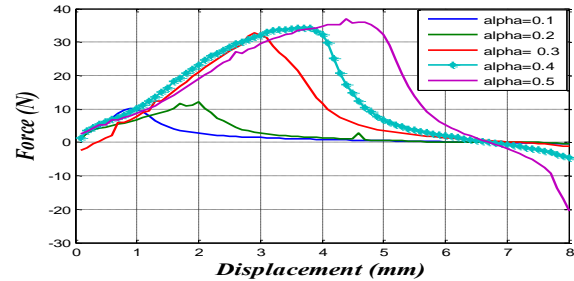


Figure 5: Stator and translator teeth width influence

Figure 5 shows the influence of the ratio  $\alpha$  on the developed force by the motor. We can conclude that:  $\alpha = 0.4 \Rightarrow W_{sp} = W_{tp} = 4mm$  is the optimum value to have a maximal force. This result confirms the obtained value in previous work [1],[3] and [10].

#### 4.2 Translator and stator yokes tickness 2D-FEA analysis

The yokes thickness of the stator and the translator are useful to canalize magnetic flux lines. That is in order to improve the optimum size and lighten the weight, the 2D-FEA is performed at lower values than  $\lambda$

( $C_y = 0.3 * \lambda, C_y = 0.5 * \lambda, C_y = 0.8 * \lambda, C_y = \lambda$ ).

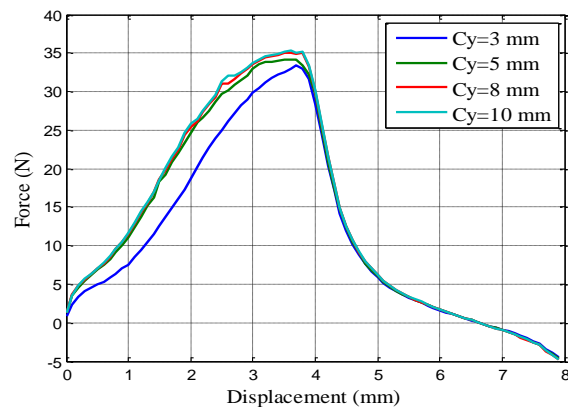


Figure 6: stator and translator yoke thickness influence

The other parameters are set constant:  
 ( $h_t = 25mm, h_s = 5mm, g = 0.1mm, \alpha = 0.4,$   
 $w_{ss} = 9.3mm, w_{ts} = 6mm$ )

Figure 6 shows the stator and translator yoke tackiness influence for a constant current density and the other geometrical parameters are fixed. The force generated by the actuator is not affect by increasing stator and translator yoke thickness when those later are higher than the half of tooth pitch  $C_y = 0.5 * \lambda$ .

In order, to minimize the weight we choose  $C_y = 5mm$

### 4.3 2D-FEA translator height teeth

The excitation coils are inserted into the translator slot width. The influence of the translator teeth height is studied in this part by 2D-FEA to show its effect in the force developed by the actuator. The values of  $h_t$  is very important because it connected to the space reserved for the coil.

$$S_C = K_{bob} \frac{S_{bob}}{N} \quad (13)$$

$$S_{bob} = l_{bob} * b_{bob} \quad (14)$$

$$N = \frac{l_{bob} * b_{bob} * K_{bob}}{S_C} \quad (15)$$

$S_C$ : Section of copper wire ( $mm^2$ ),  $K_{bob}$ : coil Fill factor of,  $S_{bob}$ : Surface occupied by the coil ( $mm^2$ ),  $b_{bob}$ : coil width ( $mm$ ),  $l_{bob}$ : coil height ( $mm$ ),  $N$ : Number of turn.

As shown in Equation 3 more the value of the stator slot depth is increasing, the coil number turns increasing too consequently, the value of the force is more important

In this stage the value investigated of teeth height are:

$$l_s = \lambda, l_s = 2 * \lambda, l_s = 2.5 * \lambda \text{ and } l_s = 3 * \lambda$$

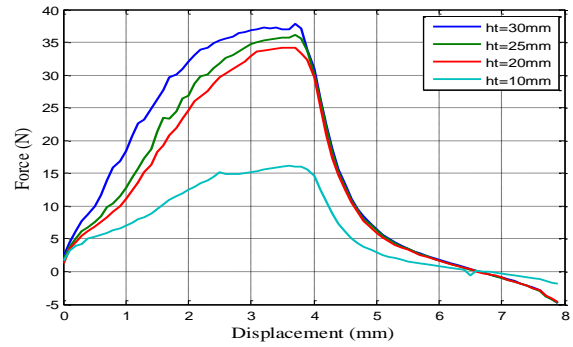


Figure 7: translator teeth height influence

Figure 7 shows the influence of translator teeth height for constant current density when the other geometrical parameters are fixed. ( $C_y = 5mm, h_s = 5mm, g = 0.1mm, \alpha = 0.4, w_{ss} = 9.3mm, w_{ts} = 6mm$ )

The gain of force decreases for higher values than  $l_s = 2 * \lambda$  so in order to not give more weight for the mobile part we choose  $l_s = 2.5 * \lambda = 25mm$ .

### 4.4 2D-FEA stator height teeth

In this part we study the height teeth stator influence. Other geometric parameters and current density are held constant.

$$(h_t = 25mm, C_y = 5mm, g = 0.1mm, \alpha = 0.4, w_{ss} = 9.3mm, w_{ts} = 6mm)$$

The  $h_s$  values investigated are lower than the tooth pitch value.  $l_m = [2mm, 10mm]$

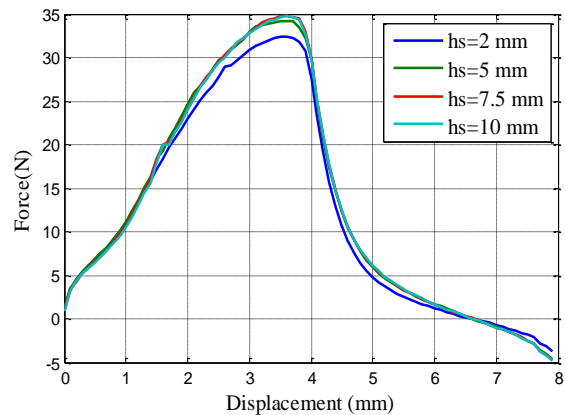


Figure 8. Stator height teeth Influence

Figure (8) shows the stator height teeth influence

where we can conclude that this parameter has no influence on the force for value higher than the half of tooth pitch therefore so we choose  $l_m = 5mm$

### 4.5 Air gap Influence

The air gap separating the moveable and a stator tooth is a mechanical parameter that is imposed by the quality of the motor manufacturing and translation guide systems. This latter has a great influence on the developed force by the actuator so in this part we study this influence by the FEA-2D

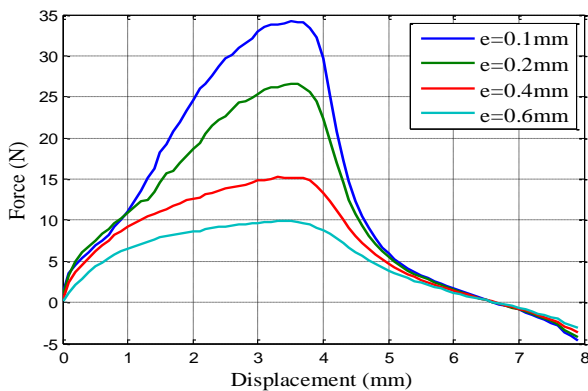


Figure 9: Air gap influence of the

As shown in figure 9 the air gap is important parameter that has a great influence on the force generated by the motor.  $e = 0.1mm$  is a suitable value.

### 4.6 Winding design

The conductor section is calculated as,

$$S_c = \frac{I_p}{j\sqrt{m}} = \frac{2}{6.4*\sqrt{4}} = 0.1563mm^2 \quad (16)$$

The winding turn number is calculate as,

$$N = \frac{l_{bob} * b_{bob} * K_{bob}}{S_c} = \frac{24 * 2.5 * 0.65}{0.1563} = 253Turn \quad (17)$$

### 4.7 Final dimension

To design a linear actuator it is important to choose the parameters that allow the maximum development of force. Table 1 summarizes various geometric parameters and characteristics of the coils

that ensure an optimal choice of force per volume unit.

We can conclude that the different geometric parameters obtained by the two proposed method are nearly equal.

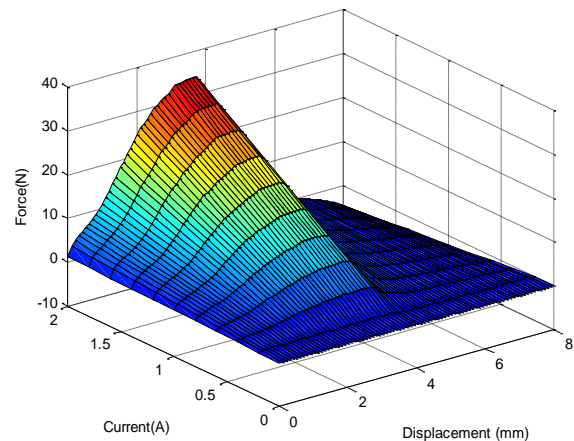


Figure 10: Force response surface as function of position and current.

Table 1: LSRM final dimension

	Parameters	Symbol	2D-FEA Value	RSRM to LSRM value
Translator	Yoke thickness	$C_{ty}$	5 mm	4mm
	Teeth width	$w_{tp}$	4 mm	4mm
	Slots width	$w_{st}$	6 mm	6mm
	Teeth height	$h_t$	25 mm	27.25mm
Stator	Yoke trickiness	$C_{sy}$	5 mm	4mm
	Teeth width	$w_{sp}$	4 mm	4mm
	Slots width	$w_{ss}$	9.3 mm	9.3
	Teeth height	$h_t$	5mm	7.6mm
Coil	Number of turn	$N$	253	253
	Section of copper wire	$S_c$	$0.153 mm^2$	$0.153 mm^2$

These three-dimensional graphs represented in figure 10 and11 show the force characteristics and fluxes as function of the displacement for different current values .Obtained results show two extreme values correspond in fact to the aligned and unaligned positions of the mover and translator teeth. Clearly, the shape and the amplitude of the thrust force are characterized by an asymmetry caused by the saturation level when the mobile

move.

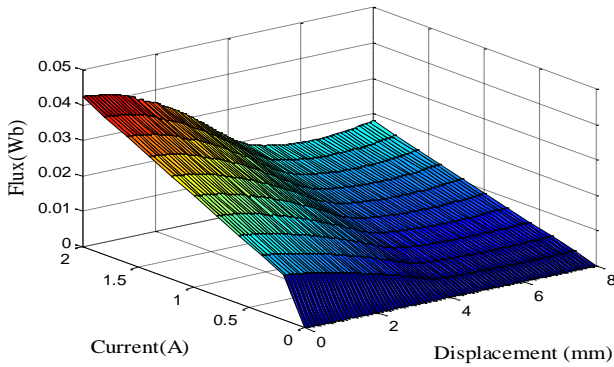


Figure 11: Flux response surface as function of position and current

The inductance profile is shown in figure 12 as function of the displacement for different current values. We can see that inductance shape is characterized by one minimum value when the mover and stator are unaligned whatever the value of the current.

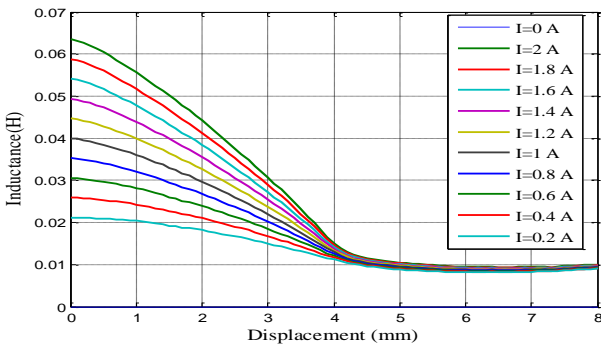


Figure 12. Inductance as function of position for different current values.

### 5 LSRM modeling

The LSRM has a high nonlinear characteristic due to its nonlinear flux behaviour [13]. In order to simplify equations, the modelling is performed without taking into account magnetic saturation, phases are considered identical and end effect is neglected [13].

Consequently, the corresponding voltage equation neglecting the mutual is given by: [10] [11] [12]:

$$u = Ri + \frac{d\phi(i, x)}{dt} = Ri + L \frac{di}{dt} + i_n \frac{di}{dt} \frac{dx}{dt} \quad (18)$$

Where  $u$  is the applied voltage,  $i$  is phase current,  $R$  is the phase resistance,  $L$  is the phase inductance,  $\phi$  is the phlox inductance.

The phase inductance is a function of position and phase current as shown in figure 12. The phase inductance as function of position with first Fourier terms is given by:

$$L_\lambda(x) = L_0 + L_1 \cos\left(\frac{2\pi x}{\lambda}\right) \quad (19)$$

Where:

$$L_0 = \frac{L_{\max} + L_{\min}}{2} = \frac{0.063 + 0.01}{2} = 0.0365H$$

$$L_1 = \frac{L_{\max} - L_{\min}}{2} = \frac{0.063 - 0.01}{2} = 0.0265H$$

The forces generated by each phase of the motor are determined as follow:

$$\begin{aligned} F_{emA} &= -\frac{1}{2} i_A^2 L_1 \frac{2\pi}{\lambda} \sin\left(\frac{2\pi}{\lambda} x\right) \\ F_{emB} &= -\frac{1}{2} i_B^2 L_1 \frac{2\pi}{\lambda} \sin\left(\frac{2\pi}{\lambda} x - \frac{\pi}{2}\right) \\ F_{emC} &= -\frac{1}{2} i_C^2 L_1 \frac{2\pi}{\lambda} \sin\left(\frac{2\pi}{\lambda} x - \pi\right) \\ F_{emD} &= -\frac{1}{2} i_D^2 L_1 \frac{2\pi}{\lambda} \sin\left(\frac{2\pi}{\lambda} x - \frac{3\pi}{2}\right) \end{aligned} \quad (20)$$

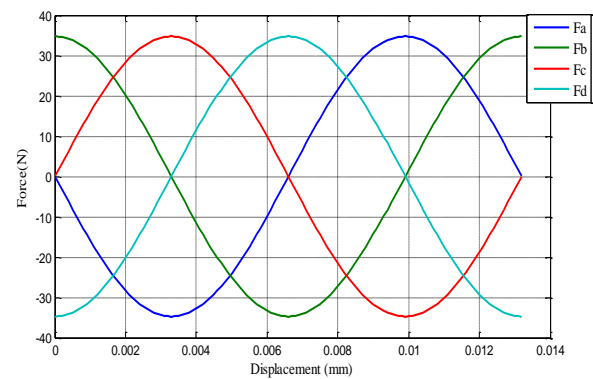


Figure 13: Theoretical force generated by the actuator

Figure 13 shows the theoretical force determined by equations 20 over the entire length of tooth pitch  $\lambda$ . We can see the sinusoidal shape which is characterized by increasing zone and decreasing zone.

So the excitation sequence of the deferent phases must take into account this consideration

$$x \in \left[ 0 \rightarrow \frac{\lambda}{4} \right] \Rightarrow \frac{\partial F_A}{\partial t} > 0$$

$$x \in \left[ \frac{\lambda}{4} \rightarrow \frac{\lambda}{2} \right] \Rightarrow \frac{\partial F_B}{\partial t} > 0$$

$$x \in \left[ \frac{\lambda}{2} \rightarrow \frac{3\lambda}{2} \right] \Rightarrow \frac{\partial F_C}{\partial t} > 0$$

$$x \in \left[ \frac{3\lambda}{2} \rightarrow \lambda \right] \Rightarrow \frac{\partial F_A}{\partial t} > 0$$

Tableau 2: Excitation sequence

	Phase A	Phase B	Phase C	Phase D
$0 \rightarrow \frac{\lambda}{4}$	Active	inactive	inactive	inactive
$\frac{\lambda}{4} \rightarrow \frac{\lambda}{2}$	inactive	Active	inactive	inactive
$\frac{\lambda}{2} \rightarrow \frac{3\lambda}{2}$	inactive	inactive	Active	inactive
$\frac{3\lambda}{2} \rightarrow \lambda$	inactive	inactive	inactive	Active

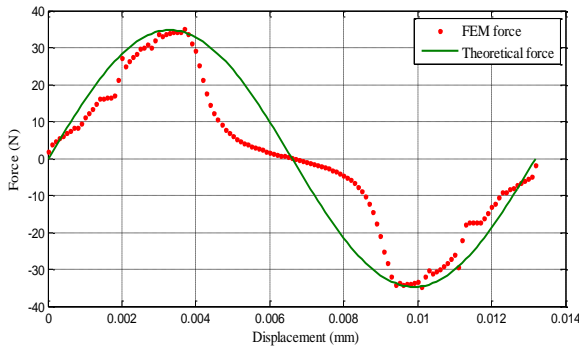


Figure 14: Theoretical and FEA force generated by the actuator

Figure 14 shows force determined by equations 20 and determined by finite element analyzes over the entire tooth pitch length  $\lambda$  the main difference comes from the choice of the mathematical model, specifically the inductance model (19). We expect that the accuracy may be improved by introducing higher order harmonics in (19) and eventually by correctly choosing the number of Fourier terms.

Finally the voltage and mechanical equations are:

$$u_A = Ri_A + L_0 \frac{di_A}{dt} + L_1 \cos\left(\frac{2\pi x}{\lambda}\right) \frac{di_A}{dt} + \frac{2\pi}{\lambda} L_1 \sin\left(\frac{2\pi x}{\lambda}\right) v i_A \tag{21}$$

$$u_B = Ri_B + L_0 \frac{di_B}{dt} + L_1 \cos\left(\frac{2\pi x}{\lambda} - \frac{\pi}{2}\right) \frac{di_B}{dt} + \frac{2\pi}{\lambda} L_1 \sin\left(\frac{2\pi x}{\lambda} - \frac{\pi}{2}\right) v i_B \tag{22}$$

$$u_C = Ri_C + L_0 \frac{di_C}{dt} + L_1 \cos\left(\frac{2\pi x}{\lambda} - \pi\right) \frac{di_C}{dt} + \frac{2\pi}{\lambda} L_1 \sin\left(\frac{2\pi x}{\lambda} - \pi\right) v i_C \tag{23}$$

$$u_D = Ri_D + L_0 \frac{di_D}{dt} + L_1 \cos\left(\frac{2\pi x}{\lambda} - \frac{3\pi}{2}\right) \frac{di_D}{dt} + \frac{2\pi}{\lambda} L_1 \sin\left(\frac{2\pi x}{\lambda} - \frac{3\pi}{2}\right) v i_D \tag{24}$$

$$\frac{dv}{dt} = -\frac{\pi L_1}{m \lambda} \left[ i_A^2 \sin\left(\frac{2\pi}{\lambda} x\right) + i_B^2 \sin\left(\frac{2\pi}{\lambda} x - \frac{\pi}{2}\right) + i_C^2 \sin\left(\frac{2\pi}{\lambda} x - \pi\right) + i_D^2 \sin\left(\frac{2\pi}{\lambda} x - \frac{3\pi}{2}\right) \right] - \frac{\xi}{m} v - \frac{F_c}{m} - \frac{F_0}{m} \text{signe}(v) \tag{25}$$

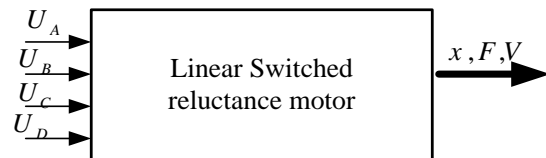


Figure 15: LSRM open loop control

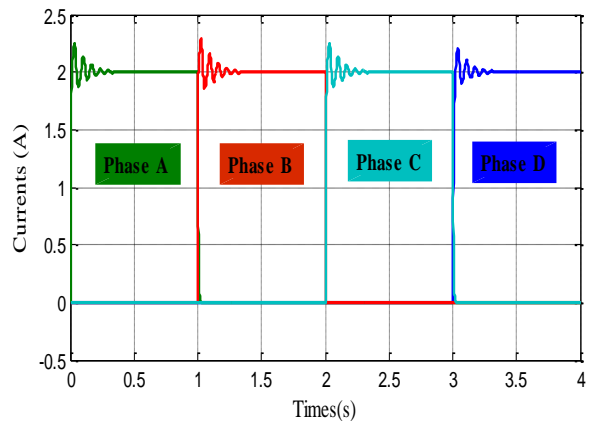


Figure 16: Phases currents

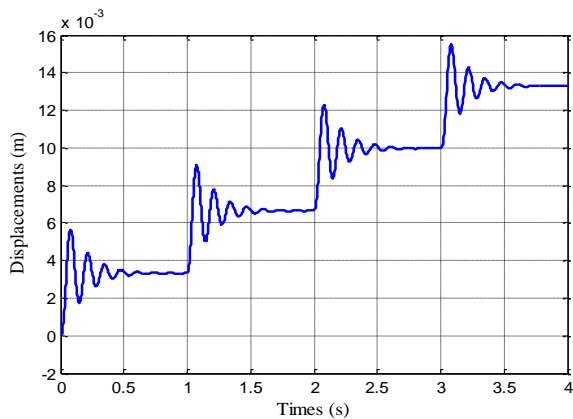


Figure 17: Displacement of the mover as function of time for 4 steps

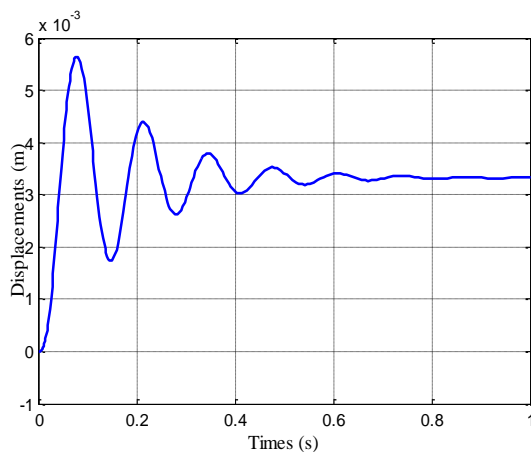


Figure 18: Displacement of the mover for 1 step

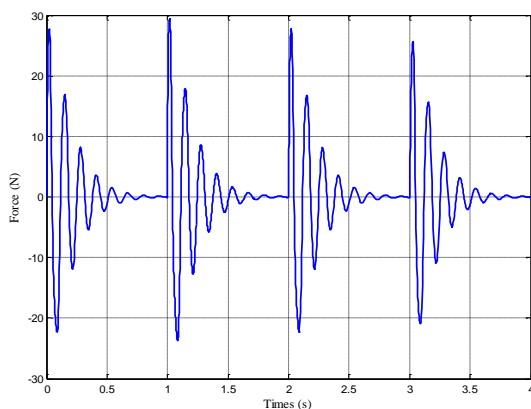


Figure 19: Force generated by the actuator

In order to show the actuator dynamic and to test the developed models, MATLAB/ SIMULINK was used as a simulation tool. The different phases are separately excited for a constant period. The period of each step is 1 second.

Figure (14) shows the phase current when just one phase is supplied for 1 second in every step

The mover displacement shown in figure (17) for four steps and figure (18) for one step prove that the motion is characterized by great over-shoot and strong oscillations. The oscillations are also observed in force in figure 19.

The oscillation observed in force and displacement are the major disadvantage of the LSRM open loop control so including this actuator into high precision application need the closed loop control by using controller and motion sensor.

## 5 CONCLUSION

This work presents a design of a single sided transverse flux linear switched reluctance motor with an active translator and a passive stator. Novel design procedure for linear switched reluctance machine has been proposed using the current knowledge design of rotary switched reluctance machines. A finite element study is carried out to show the geometric parameters influence on the generated force by the actuator. Obtained results are compared to confirm the efficiency of the proposed design method for an optimum design with an optimum force characteristic per unit volume. The second parts of this work devoted to the modelling of the LSRM neglecting the saturation and present the actuator dynamic on open loop control. The main feature of the studied device consists of ensuring a direct motion without the need for traditional gear so included in high precision applications.

### References:

- [1]. Khidiri J, *Alimentation et commande d'un actionnaire linéaire triphasé flux transversale*, These de Docteur Ingénieur, Université des Sciences et Techniques de Lille Flandres-Artois, 1986.
- [2]. Byeong-Seok Lee, Han-Kyung Bae, Praveen Vijayraghavan and R. Krishnan, Design of a Linear Switched Reluctance Machine *IEEE TRANSACTION ON INDUSTRIAL APPLICATION*, VOL.36, NO 6, Novembre/December 2000
- [3]. J.G Amoros, and P. Andrada, Sensitivity Analysis of Geometrical Parameters on a Double-Sided Linear Switched Reluctance

- Motor, *IEEE TRANSACTIONS ON INDUSTRY APPLICATIONS*, VOL. 57, NO. 1, JANUARY 2010
- [4]. Zaafrane Wajdi, Kediri Jalel And Rehaoulia Habib, Sliding Mode Current Control of Linear Switched Reluctance Motor, *international Journal of Emerging Science*, Vol 3(2), 130-143, June 2013
- [5]. Byeong-Seok Lee, *Linear Switched Reluctance Machine Drives with Electromagnetic Levitation and Guidance Systems*, PHD thesis, Blacksburg, Virginia, 2000.
- [6]. Mr. Myo Min Thet, Design and Calculation of 75W Three-phase Linear Switched Reluctance Motor *World Academy of Science, Engineering and Technology*, Motoring And Technology Volume 36,2070-3740, 2008.
- [7]. S.S. Murthy, Bhim Singh and Virendra Kiimar Sharma, Finite element analysis to achieve optimum geometry of switched reluctance motor in Proc, *IEEE TENCON*, vol 2, pp.414-418,2008.
- [8]. J Faiz, JW Finch, Aspects of design optimization for switched reluctance motors, *IEEE Transactions on Energy Conversion*, Vol. 8, No. 4, December 1993
- [9]. N. K. Sheth and K. R. Rajagopal, Optimum pole arcs for a switched reluctance motor for higher torque with reduced ripple, *IEEE International on Magnetics*, VOL. 39, NO. 5, SEPTEMBER 2003.
- [10]. KANT M, *Les actionneurs électriques pas à pas*, Edition Herms, Paris, 1989 .
- [11]. Chevailler.S. *Comparative study and selection criteria of linear motor*, PHD thesis. Ecole Polytechnique Fédérale de Lausanne la facult Sciences et Techniques de l'Ingénieur, Laboratoire d'actionneur integers, 2006 .
- [12]. MAHMOUD Imed, REHAOULIA Habib and AYADI Mahfoudh : Design and modelling of a linear switched reluctance actuator for biomedical applications *International Journal of the Physical Sciences*, Vol 6(22), 2, 2011 .
- [13]. Ghislain REMY : Commande optimise d'un actionneur linaire synchrone pour un axe de positionnement rapide PHD thesis. Ecole Doctorale n 432, Sciences des Mtiers de l'Ingénieur, 2007.
- [14]. L. Kolomeitsev, D. Kraynov, S. Pakhomin, F. Rednov, E. Kallenbach, V. Kireev, T. Schneider, J. Bcker3, Linear Switched Reluctance Motor as a High Efficiency Propulsion System for Railway Vehicles, *SPEEDAM* pp.155-160, 2008.
- [15]. N. S. Lobo, Hong Sun Lim and R. Krishnan: Comparison of Linear Switched Reluctance Machines for Vertical Propulsion Application, Analysis, Design, and Experimental Correlation, *IEEE TRANSACTIONS ON INDUSTRY APPLICATIONS*, VOL. 44, NO. 4, 2008.
- [16]. Wajdi Zaafrane, Jalel Kediri and Habib Rehaoulia, 2-D Finite Element Design of a Single Sided Linear Planner Switched Reluctance Motor, *World Applied Sciences Journal* 25 (3): 494-499, 2013.